Experimental assessment of a phase change material in walls for heating and cooling applications

Benoit Delcroix[1], Michaël Kummert[1], Ahmed Daoud[2] and Jonathan Bouchard[2]
[1] École Polytechnique de Montréal, Montréal, Québec, Canada
[2] Laboratoire des Technologies de l'Énergie, Hydro-Québec Research Institute, Shawinigan, Québec, Canada

Abstract

The performance of a bio-based phase change material (PCM) was experimentally investigated in two identical full scale test huts exposed to the exterior environment. A layer of PCM enclosed in protective lightweight plywood sheets were added on the inside of 50 % of the walls (excluding floor and ceiling) in one of the test huts. Five months of data were recorded in 2013, from the end of February to the end of July. Several scenarios were tested for heating and cooling applications and clear differences were observed between both huts. The results show that adding PCM to building walls mitigates temperature variations and produces a time shift of wall temperature extremes. Data was also used to benchmark an EnergyPlus simulation model of the test huts.

1 Introduction

In Quebec, the main energy source for space conditioning is electricity. Electric space heating is present in more than two thirds of households and approximately 60 % of the commercial and institutional (CI) sectors. During winter, the combined space heating load from the residential and CI sectors can contribute to 40 % of the total electricity peak demand (Leduc et al. 2011). Figure 1 presents the evolution of the average power demand on the electric grid in Quebec in winter (January) and summer (July). It shows the important seasonal and daily profile differences.

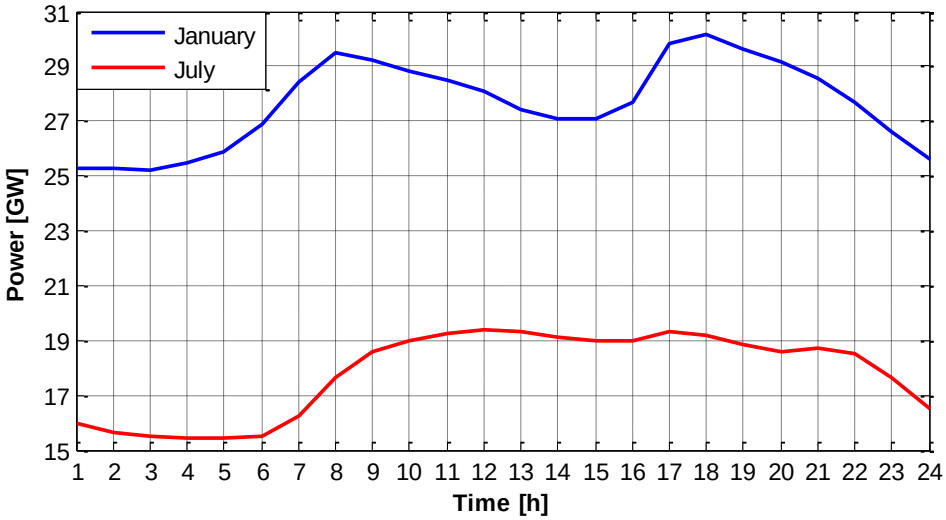

Figure 1: Prediction of the average hourly power demand in the province of Quebec in January and July 2007 (Hydro-Québec 2006)

During a typical winter day in Quebec, morning and evening peaks are present, roughly corresponding to the beginning and the end of regular working days. During summer months, the

power demand has a flatter profile during regular working hours because the load is dominated by lighting, appliances and cooling in the CI and residential sectors.

A possible solution to mitigate the daily power peaks in winter and summer is adding thermal mass to the building using phase change materials (PCMs), which should allow shifting heating and cooling loads in time. PCMs offer unique opportunities if their high energy storage density and their nearly isothermal heat release (during phase change) are used appropriately. Several authors have reviewed the state of the art in PCMs, their properties and their possible applications (Zalba et al. 2003; Farid et al. 2004; Sharma et al. 2009; Baetens et al. 2010; Mehling & Cabeza 2008). Some models were developed to simulate the PCM behaviour in different applications, namely for a water tank with embedded PCM (Bony & Citherlet 2007; D'Avignon & Kummert 2013) and for PCMs embedded within walls or slabs (Ibánez et al. 2005; Dentel & Stephan 2010; Kuznik et al. 2010). These models use the effective heat capacity method (Goodrich 1978; Yao & Chait 1993) or the enthalpy method (Voller & Cross 1981) to represent the physical processes within PCMs. Both methods allow taking into account the variable heat capacity (as a function of temperature) of PCMs. However, only a few models are able to represent the hysteresis and subcooling effects of PCMs (Günther et al. 2009). The hysteresis is the temperature difference between the melting and solidification temperatures. The subcooling effect consists in the cooling of the liquid phase below this solidification temperature, before the phase change takes place.

This paper focuses on the experimental assessment of the use of PCM during heating and cooling periods. In addition, test huts measured and simulated data is compared to an EnergyPlus (Crawley et al. 2001) model using the PCM module (Pedersen 2007; Tabares-Velasco et al. 2012) with the enthalpy method. Implementation of the PCM in the EnergyPlus model is also addressed.

2 Experimentation

PCM properties and arrangement

The selected material is a bio-based PCM (biodegradable and composed of soybean and palm oils) with a phase change temperature of 23 °C. It is mixed with a gelling agent. The main properties and a picture of the product (embedded within plastic-film pouches) are presented in Figure 2.

Properties	Unit	Value
Weight per square foot	kg/m²	1.465
Melt point	°C	23
Latent heat storage capacity	J/g	165-200
Specific heat (solid)	J/(g.K)	1.84
Specific heat (liquid)	J/(g.K)	1.99
Density	kg/m³	830
Thermal conductivity (solid)	W/(m.K)	0.207
Thermal conductivity (liquid)	W/(m.K)	0.171

Figure 2: Container and properties of the used PCM

A differential scanning calorimetry (DSC) test was performed on the PCM. Figure 3(a) presents the evolution of the heat flow as a function of temperature. Positive and negative heat flows respectively correspond to heat release (cooling process) or absorption (heating process). It shows that the fusion and solidification processes occur at different temperature ranges. Solidification occurs between 15 and 20 °C while fusion occurs between 20 and 25 °C, which mean that the hysteresis is about 5 °C. Figure 3(b) presents the resultant enthalpy-temperature curve.

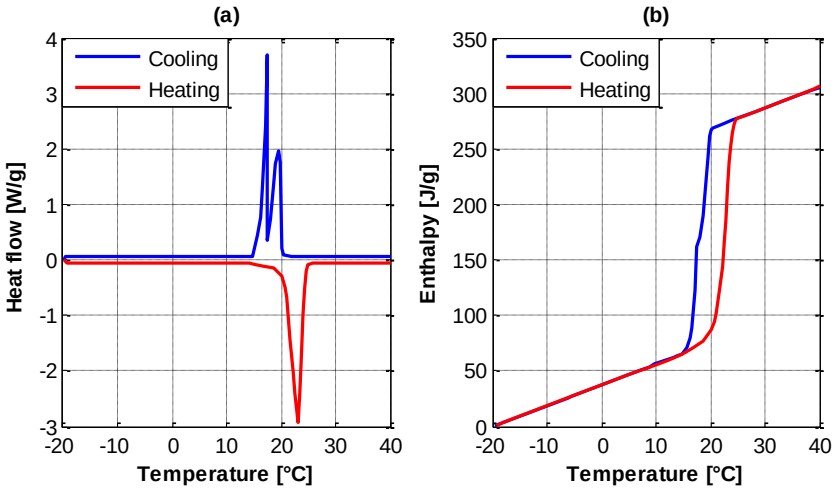

Figure 3: Differential Scanning Calorimetry (2 °C/min) test (a) and enthalpy-temperature curve (b)

PCM-equipped walls

The installation of the PCM in the test huts was conducted as presented in Figure 4. A double layer of plastic film with PCM pouches is inserted between two plywood boards (0.00635 m each). The central layer composed of PCM, plastic film and air has a thickness of 0.0175 m.

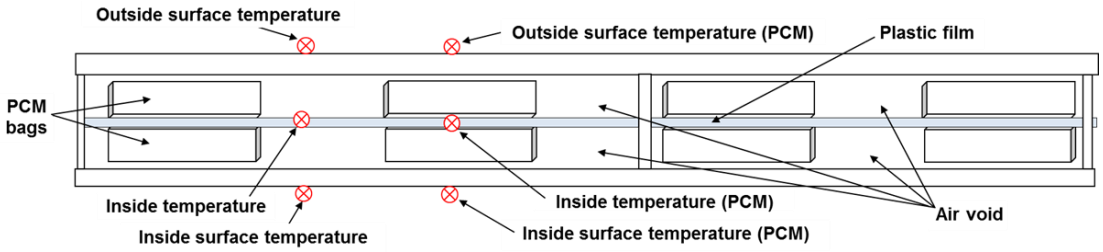

Figure 4: PCM-equipped panel (test hut with PCM)

Empty panels were also added in the other test hut (without PCM) to keep both test huts comparable. These panels were added to the inside surface of the external walls of each test hut, as presented in the following section.

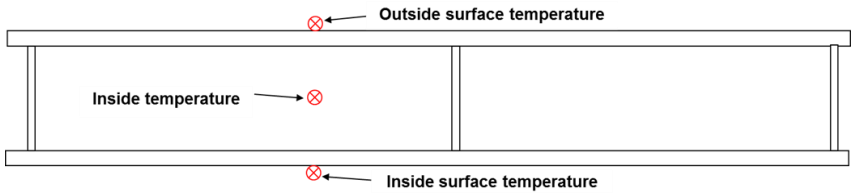

Figure 5: Empty panel (control test hut, without PCM)

Figure 4 and Figure 5 also show where thermocouples were installed within the panels and at their surfaces.

Test hut description and instrumentation

The test bench is located in Shawinigan (QC, Canada) at Hydro-Québec's Laboratory of Energy Technologies. It consists of two identical fully instrumented test huts (Figure 6). One is equipped with PCM while the other is not. Figure 6 and Table 1 describe the test huts characteristics, including the envelope U-values, the air infiltrations, the dimensions and the positions

of the added panels with or without PCMs. Both test huts are instrumented with sensors which measure air (dry bulb) temperatures (at several heights), inside surface temperatures (walls, floor, ceiling and windows), and electric energy use for heating. The added panels (with and without PCMs) are situated on the inside surface of the south-west and north-west external walls (presented in Figure 7) and are also instrumented, as shown in Figure 4 and Figure 5. A weather station is also available next to the test-bench.

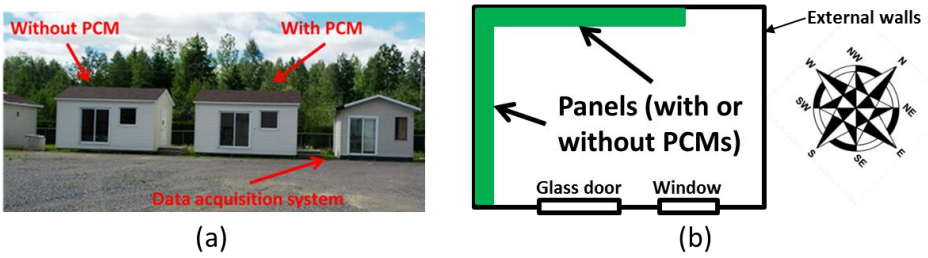

Figure 6: (a) Photo of the test bench and (b) top view of a test hut with its orientation

Table 1: U-values, infiltration and dimensions of the test hut

Surfaces	Unit	Value
Walls	W/(m²K)	0.28
Roofs	W/(m²K)	0.19
Slab	W/(m²K)	0.14
Door	W/(m²K)	1.25
Window	W/(m²K)	1.6
Glazed door	W/(m²K)	1.6
Infiltration	h^{-1}	0.1

Measures	Unit	Value
Length	m	5.49
Width	m	3.66
Height	m	2.44
Glazed door surface	m²	3.91
Window surface	m²	1.19

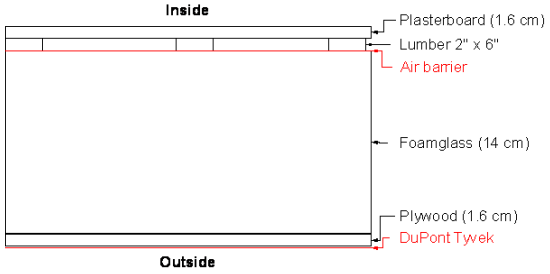

Figure 7: External wall

Tests description and results

Tests took place from the end of February to the end of July 2013. During the heating season, temperature set-point scenarios were tested. During the cooling season, the temperature in the test huts was allowed to float. Table 2 presents the different scenarios. This paper focuses on presenting the results of two scenarios: the residential and CI scenarios for heating.

Table 2: Tested scenarios

Scenario	Date	Set-point			
Constant set-point	28-02 → 11-03	23 °C			
Residential workday set-point	11-03 → 22-03	6:00 AM		4:00 PM	
		↓ 19 °C		↑ 23 °C	
Commercial and institutional (CI) set-point	25-03 → 28-03	6:00 AM		6:00 PM	
		↑ 24 °C		↓ 18 °C	
Early morning preheating set-point	28-03 → 05-04	3:00 AM	6:00 AM	9:00 AM	8:00 PM
		↑ 25 °C	↓ 20 °C	↑ 22 °C	↓ 18 °C
Extreme set-back	08-04 → 30-04	8:00 AM		8:00 PM	
		↑ 30 °C		↓ 5 °C	

Figure 8(a) compares the evolution of the temperatures of the indoor room air and in the center of the panel for the test hut with PCM and the control test hut (without PCM) for the residential scenario during two days (17-03 and 18-03). During the day, solar radiation overheats the test huts and the indoor air temperature rises significantly. In the PCM test hut, the PCMs allow mitigating the temperature increase by 2 °C by storing more energy in the walls. The temperature difference at the panel center is significant, showing the impact of PCMs on the wall transient response. The panel center temperature during the night is stabilized around 19 °C for the control test hut while it takes about 6 to 7 more hours for the panel center temperature in the PCM test hut to decrease to 19 °C.

Figure 8(b) presents the evolution of the heating power (mean power over a 15-min time-step) in both test huts. At 6 AM, when the set-point is reduced from 23 °C to 19 °C, the heating system is turned off during a few moments (the test huts have very little thermal mass). Afterwards, it is turned on just to maintain the set-point of 19 °C. At this moment, the power demand is more important in the control test hut due to less stored heat in the walls (in comparison with the PCM test hut). At the end of the day, when the set-point is set again to 23 °C, the heating system is turned on to match the set-point. Because of its higher thermal mass (and for charging energy in the PCMs), the PCM test hut needs more power than the control test hut to reach the set-point, as shown at the end of the afternoon on Figure 8(b). Finally, during the night, as the wall temperature in the PCM test hut decreases more slowly, the heating power is less important than in the control test hut where the wall temperature has already reached a colder state.

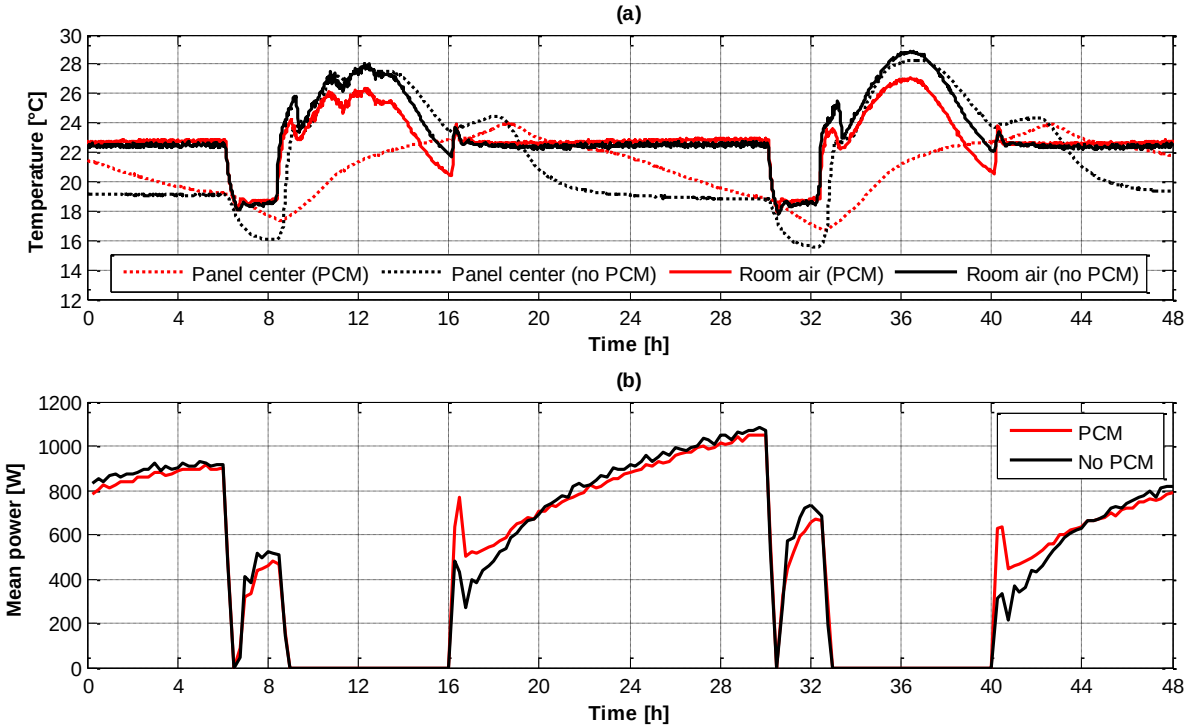

Figure 8: (a) Evolution of temperatures inside the test huts and in the center of the panels (with and without PCMs) and (b) evolution of the heating power during residential workday scenario (17-03 and 18-03)

Figure 9 presents the same results for the CI scenario. The effects of temperature peak mitigation and delay that were visible in Figure 8(a) are also present in Figure 9(a). The phase change effect appears here clearly at the end of the day, around 8 PM. The temperature slope decreases significantly at this moment.

The heating power demand (Figure 9(b)) shows two main differences. First, the power demand during the night is different: in the PCM test hut, the heating system turns on later and then delivers a lower heating power, which can be explained by the slow temperature decrease in the PCM panel at this moment (especially in comparison with the empty panel in the control test hut). On the other hand, the heating system needs to be slightly turned on at the end of the afternoon in the PCM test hut to maintain the set-point of 24 °C, which is not the case in the control test hut where the solar radiation has overheated the zone during the day.

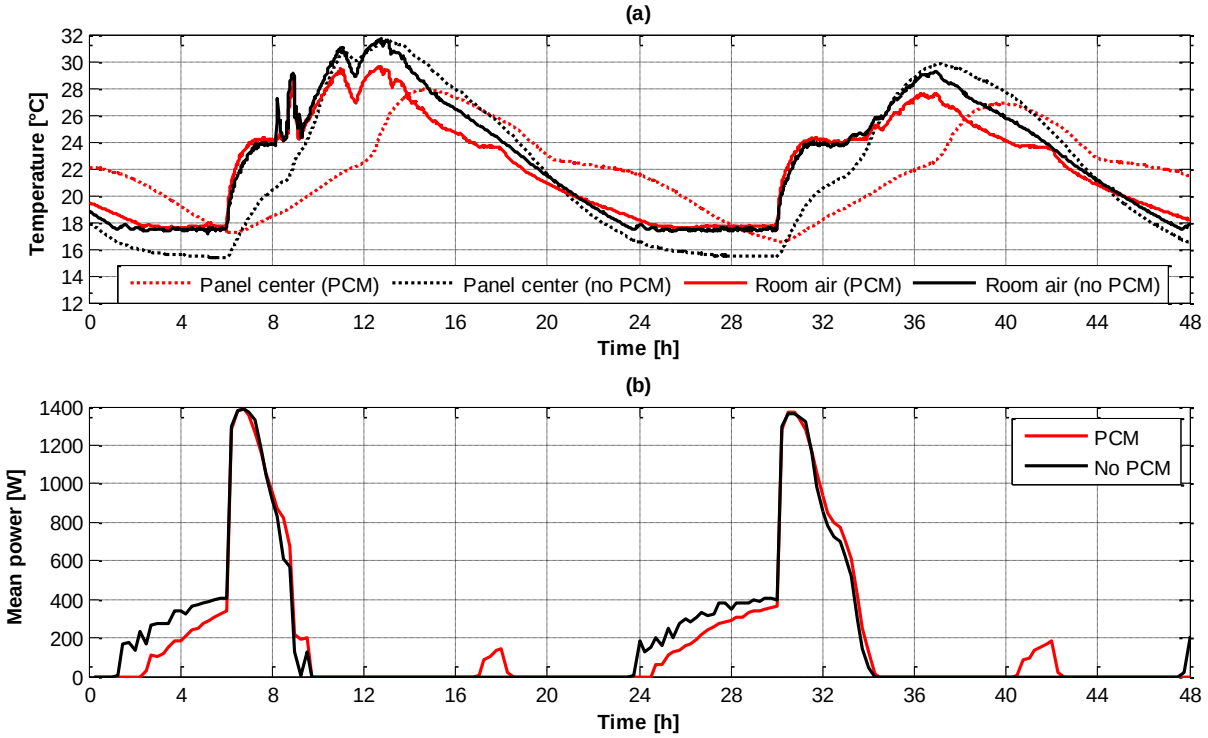

Figure 9: (a) Evolution of temperatures inside the test huts and in the center of the panels (with and without PCMs) and (b) evolution of the heating power during CI scenario (26-03 and 27-03)

The detailed temperature measurements within the walls showed two other interesting effects.

First, the temperature gradient inside a wall is strongly different, as shown in Figure 10. It presents the evolution of air and panels temperatures during the extreme set-back scenario (without (a) and with (b) PCMs). Figure 10(a) shows moderate temperature gradients since all temperatures are relatively close. PCM walls (Figure 10(b)) show a different dynamic response. The increased latency makes the panel center the coldest spot (for a short time) during a temperature rise while it becomes the warmest point (for a longer period) during a temperature fall.

A second observable effect is the appearance of an inhomogeneous temperature pattern inside the panel center due to the heterogeneity of the central layer composed of air, PCMs and a small amount of plastic film (Figure 11). During the test, measurements at the level of the PCMs pouches and in the air spaces besides the pouches were carried out as shown in Figure 4. Two measurement points were also placed at the level of the inside surface to evaluate if the thermal heterogeneity was extended to the inside surface. A significant difference is observed in the panel center (especially during the phase change (around 21 - 23 °C)). Otherwise, it seems that this thermal heterogeneity is mitigated at the level of the inside surface as no significant difference is visible.

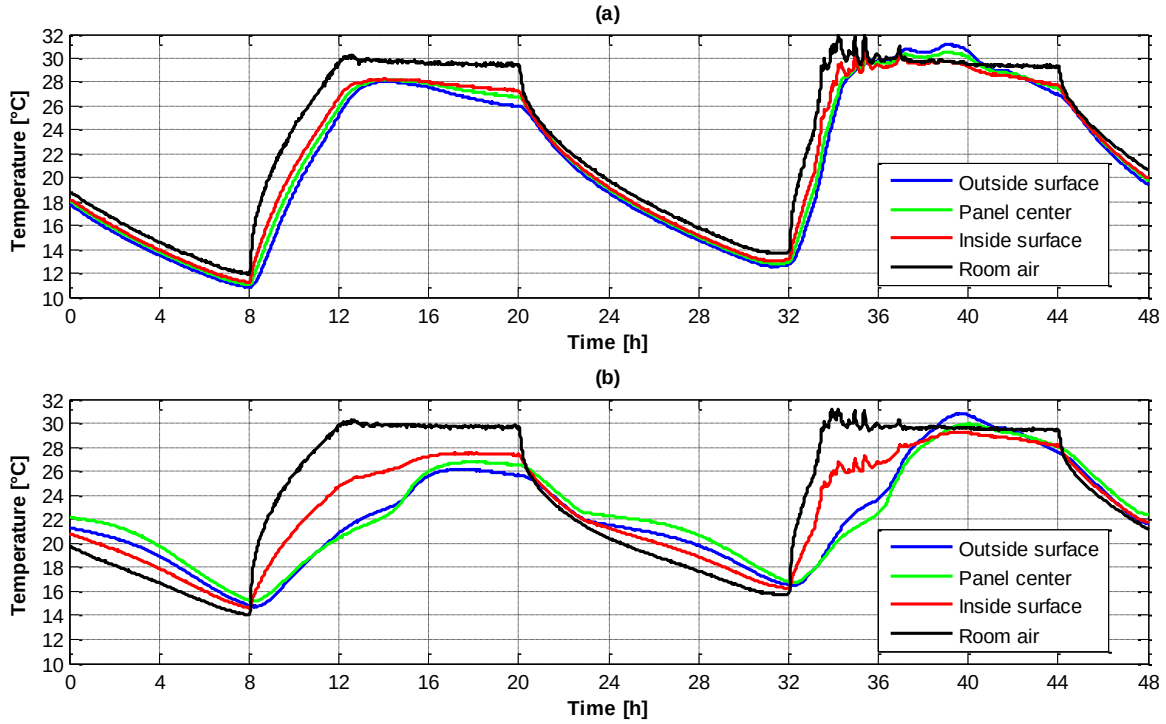

Figure 10: Evolution of the temperature gradient in the panel without (a) and with (b) PCM during the extreme set-back scenario (13-04 and 14-04)

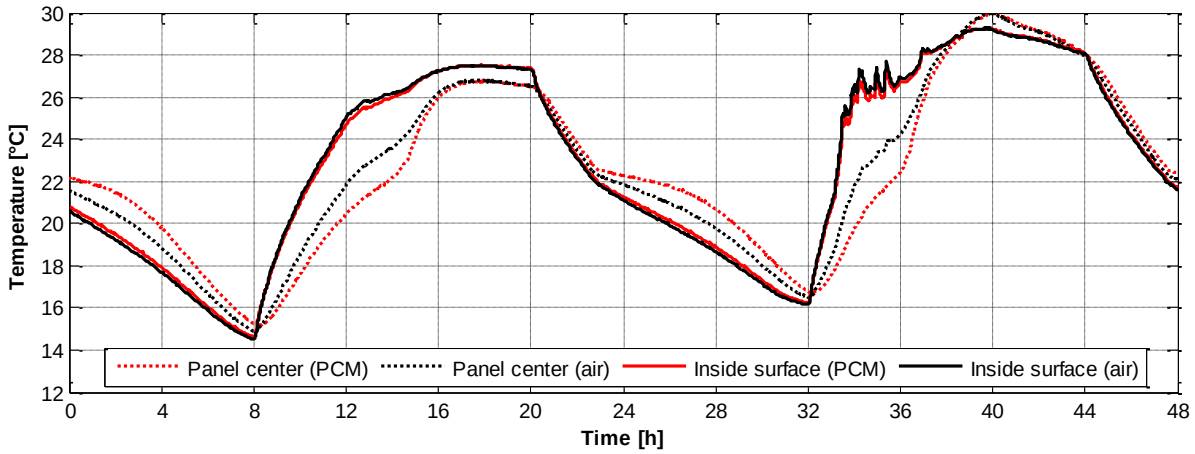

Figure 11: Illustration of the temperature heterogeneity in the panel center (with PCM) (13-04 and 14-04)

During the tests, heating consumption of both test huts was also recorded for each scenario. Figure 12 shows that the difference between test huts with and without PCMs is relatively small (less than 3 %), except for the CI scenario. The combined effect of solar radiation and a higher set-point during the day allowed storing more energy, leading to a reduced heating use during the night.

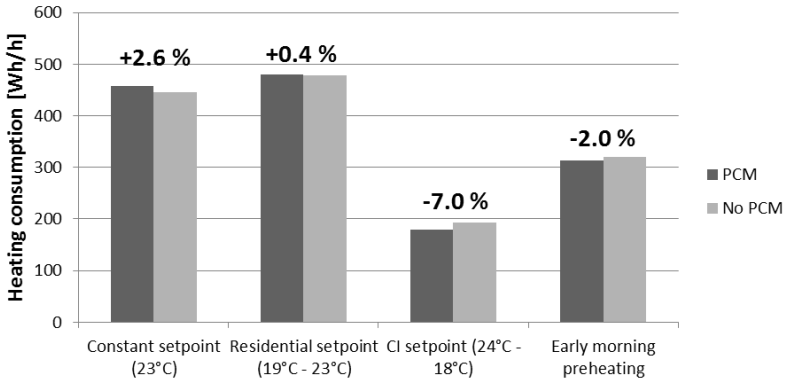

Figure 12: Heating consumption for different scenarios with and without PCM

3 Models

This section first presents the benchmarking procedure for an EnergyPlus model of the test huts without PCMs. The method used to implement a layer of PCMs in the building model is then presented. A comparison between measured and simulated data (with PCMs) is finally described and analyzed.

Control hut model and benchmarking

A building model was implemented in EnergyPlus to represent the test huts described above. The benchmarking process allowed to fine-tune some parameters of the model using the test huts measured data. Figure 13 presents some results for the indoor room temperature during the extreme set-back scenario. As shown in the figure, the modelled room air temperature is relatively close to the experimental results (obtained with the sensor located at mid-height), especially during the temperature fall and rise. However, the simulated data underestimates slightly the minimum indoor room temperature (maximum around 1 °C). This calibrated model (without PCMs) was used as a starting point to model the test hut with PCMs.

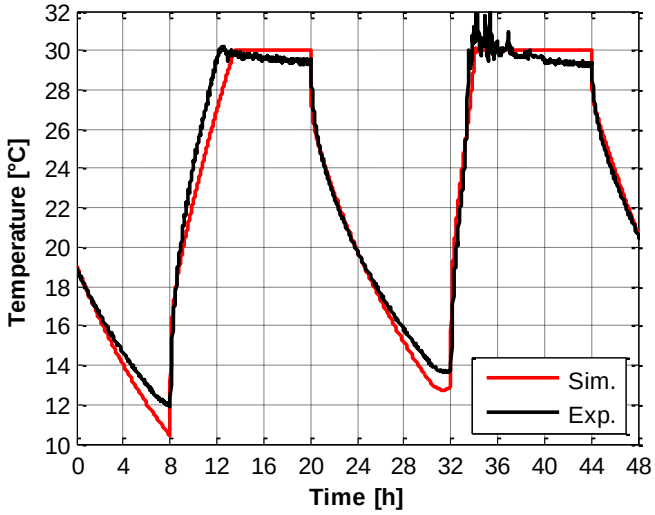

Figure 13: Comparison between simulated and measured indoor room temperatures in the test hut without PCM during the extreme set-back scenario (from 12-04 to 14-04)

PCM modeling

As mentioned above, EnergyPlus models the PCMs using the enthalpy method, which is combined to a state-space representation of the other layers within the wall. Only one enthalpy-

temperature curve can be implemented, so the model does not allow taking into account the hysteresis and subcooling effects of a PCM. The simulations were then run twice with both enthalpy-temperature curves, as described below.

As the PCM layer cannot be represented perfectly in 1-D (see Figure 2 and Figure 4), two possible ways were tested to integrate PCMs in the building model. First the central layer (air, PCMs and plastic film) of the panels is considered as an equivalent layer (Figure 14(a)). Secondly the central layer is split in several uniform layers of PCMs and plastic film while ignoring the air (Figure 14(b)), as suggested by Muruganantham (2010). This last method does not require pre-data-treatment to calculate the equivalent properties of the central layer. Table 3 gives the properties of all the layers shown in Figure 14.

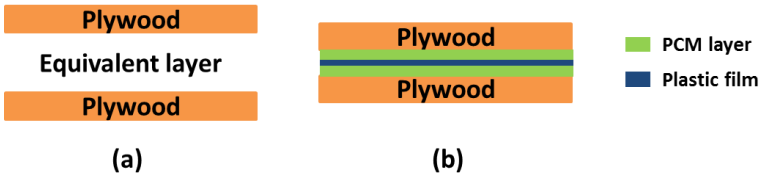

Figure 14: Schematic view of the two tested ways to model PCM layer

Table 3: Properties of the different layers

Material	Thickness [m]	Thermal conductivity [W/(m.K)]	Density [kg/m³]	Specific heat [J/(g.K)]
Plywood	0.00635	0.150	850	1250
Equivalent layer	0.0175	0.742 (solid) - 0.645 (liquid)	218	Variable
Plastic film	0.001	0.150	900	1800
PCM	0.00175	0.207 (solid) - 0.171 (liquid)	830	Variable

In the case of the equivalent layer, determining the properties is an important step. The density was computed as the volumetric average of the densities of each material. The same method was used to calculate the equivalent (mass-weighted) specific heat, except that this step was repeated for each temperature step (because the specific heat of a PCM changes with temperature). As to the calculation of the thermal conductivity, the resistance of the thin air layer was neglected. Then the thermal resistances of the both PCM layers and the plastic film were summed to obtain the equivalent thermal resistance (for the liquid and solid states). During the phase change, the thermal conductivity has a linearly interpolated value between the solid and liquid values. The following paragraph explains mathematically how each property of the equivalent layer in Table 3 was computed.

As the weight per surface (1.465 kg/m²) and the density (830 kg/m³) of the PCM are known, the equivalent thickness L_{eq} for two layers of PCM can be found such as:

$$L_{eq} = \frac{1.465 \times 2}{830} = 0.0035 \text{ m} \quad (1)$$

As the thickness of the central layer is known (0.0175 m), the volumetric percentage of each element (plastic film, PCMs and air) of the central layer is then calculated:

$$\%_{vol,PCM} = \frac{0.0035}{0.0175} \times 100 = 20\ \% \quad (2)$$

$$\%_{vol,Plastic} = \frac{0.001}{0.0175} \times 100 = 5.7\ \% \quad (3)$$

$$\%_{\mathrm{vol,Air}} = 100 - 20 - 5.7 = 74.3\ \% \quad (4)$$

From these results, it is possible to evaluate the equivalent density ρ_{eq}:

$$\rho_{\mathrm{eq}} = 0.743 \times 1.2 + 0.2 \times 830 + 0.057 \times 900 = 218\ \mathrm{kg/m^3} \quad (5)$$

As the volumetric percentage and the density are known for each element, the mass percentage is:

$$\%_{\mathrm{mass,PCM}} = \frac{0.2 \times 830}{0.743 \times 1.2 + 0.2 \times 830 + 0.057 \times 900} \times 100 = 76\ \% \quad (6)$$

$$\%_{\mathrm{mass,Plastic}} = \frac{0.057 \times 900}{0.743 \times 1.2 + 0.2 \times 830 + 0.057 \times 900} \times 100 = 23.5\ \% \quad (7)$$

$$\%_{\mathrm{mass,Air}} = 100 - 76 - 23.5 = 0.5\ \% \quad (8)$$

The equivalent specific heat, e.g. for the solid state, is computed:

$$\mathrm{C_{ps,eq}} = 0.76 \times 1.84 + 0.235 \times 1.8 + 0.005 \times 1.01 = 1.83\ \mathrm{J/(g.K)} \quad (9)$$

Finally the equivalent thermal resistance (for solid and liquid states) is the sum of the resistances of both PCM layers and plastic film while neglecting the thin air layer:

$$\mathrm{R_{eq,s}} = 2 \times \frac{0.00175}{0.207} + \frac{0.001}{0.15} = 0.02357\ m^2K/W \quad (10)$$

$$\mathrm{R_{eq,s}} = 2 \times \frac{0.00175}{0.171} + \frac{0.001}{0.15} = 0.02713\ m^2K/W \quad (11)$$

These thermal resistances gives values of thermal conductivity for the solid and liquid states which are equal to 0.742 and 0.645 W/(m.K), respectively.

Simulation description, results and analysis

This section presents a comparison of simulated and measured results for the extreme set-back scenario. As presented in Table 4, four types of simulations were run, depending on the PCM model (Figure 14) and the enthalpy-temperature curve (Figure 3(b)). The options names (letters A to D) are used in the legend of the following figure presenting the results. As options A and C and options B and D give very similar results, only the options A and B are presented, which are the options using an equivalent layer.

Table 4: Simulation options

Name	PCM model	Enthalpy-temperature curve
A	Figure 14(a)	Cooling
B	Figure 14(a)	Heating
C	Figure 14(b)	Cooling
D	Figure 14(b)	Heating

The results presented in Figure 15 focuses on the temperature at the PCM panel center for the test hut south-west wall.

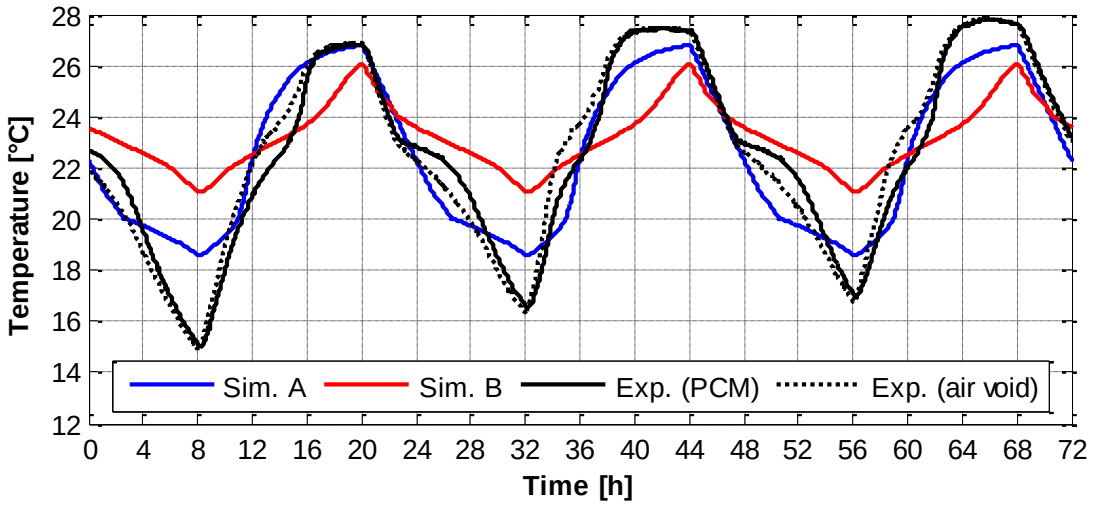

Figure 15: Comparison between simulated and measured temperature at the panel center in the test hut with PCM during the extreme set-back scenario (from 12-04 to 14-04)

Figure 15 allows highlighting two major issues. First, the simulated results over-estimate the latent heat storage capacity of PCMs since the phase change lasts significantly longer in the simulated results. Secondly, the phase change temperature ranges displayed by simulated and measured data are also significantly different. Table 5 summarizes some important properties values for the simulated and experimental data. The PCM properties implemented in the simulation parameters are those of Figure 2 and Figure 3, which are based on the DSC test. On the other hand, the properties obtained experimentally with the test huts are the result of the observation of graphs. When looking at the graph (Figure 15) the solidification temperature is clearly defined between 22 and 23 °C. The fusion temperature is more difficult to identify but a slight decrease of the curve slope is observed approximately in the same temperature range as the cooling process.

Table 5: Properties comparison

	Process	Phase change temperature range [°C]	Latent heat storage [J/g]
Simulation	Cooling	15 - 20	200
(from DSC test)	Heating	20 - 25	
Experimentation	Cooling	22 - 23 *	N/A **
(deducted from test huts)	Heating	Less perceptible but around the same as cooling *	

* Directly observed in the graphs of the temperature evolution

** As the measured values in the test huts are only temperatures we have no way to determine the latent heat storage

The main issue is then how to explain the difference observed between the results obtained with the DSC test and those shown by the test hut equipped with PCMs. As explained by Günther et al. (2009), the method (such as a DSC test) and the cooling or heating rate used to determine the PCM properties affects the test results, and especially the latent heat storage capacity and the phase change temperature range. A sensitivity analysis would then be interesting to obtain the latent heat storage capacity and the phase change temperature range which fit with the measured data.

4 Conclusions

The paper aimed at studying the contribution of the use of PCM in the building envelope by analyzing experimental data and evaluating a building simulation model of the test-bench with and without PCMs.

On one hand, measured data have shown a significant increase of the thermal mass which allows some attenuation and time shifting of the temperature extremes. In terms of peak heating demand, results have shown that PCMs offer an advantage when the set-point during the day is higher than during the night. The combined effect of the solar radiation and a higher set-point allows storing more energy in walls during the day, which delays and decreases the heating demand during the night. This effect also affects positively the heating consumption.

On the other hand, the comparison between simulated and measured results raises two important issues:

1. When a PCM with a 3-D geometry is to be modeled, care must be taken when choosing a method to model correctly the PCM in 1-D. This paper presented 2 methods which give very similar results. However, the second method (which ignores the air) requires no data pre-treatment.
2. The properties determination of the selected PCM is an important step (especially the specific heat as a function of the temperature). The comparison between the simulated results (obtained with PCM properties based on the DSC test) and the measured data have shown a poor agreement, which is due to clear differences in latent heat storage capacity and phase change temperature range.

Further research will aim at refining the different scenarios (setpoint profiles) to maximize the benefits of PCMs, and to perform a sensitivity analysis of the PCM properties in order to achieve a better match between simulated and measured data.

5 References

Baetens, R., Jelle, B.P. & Gustavsen, A., 2010. Phase change materials for building applications: A state-of-the-art review. *Energy and Buildings*, 42(9), pp.1361–1368. Available at: http://www.sciencedirect.com/science/article/pii/S0378778810001180.

Bony, J. & Citherlet, S., 2007. Numerical model and experimental validation of heat storage with phase change materials. *Energy and Buildings*, 39, pp.1065–1072. Available at: http://www.sciencedirect.com/science/article/pii/S037877880600291X.

Crawley, D.B. et al., 2001. EnergyPlus: creating a new-generation building energy simulation program. *Energy and Buildings*, 33(4), pp.319–331. Available at: http://www.sciencedirect.com/science/article/pii/S0378778800001146.

D'Avignon, K. & Kummert, M., 2013. Comparison of system-level simulation and detailed models for storage tanks with phase change materials. In *13th Conference of International Building Performance Simulation Association*. Chambéry, pp. 2940–2947.

Dentel, A. & Stephan, W., 2010. Thermal comfort in rooms with active PCM constructions. In *8th International Conference on System Simulation in Buildings*. Liège, Belgium.

Farid, M.M. et al., 2004. A review on phase change energy storage: materials and applications. *Energy Conversion and Management*, 45(9–10), pp.1597–1615. Available at: http://www.sciencedirect.com/science/article/pii/S0196890403002668.

Goodrich, L.E., 1978. Efficient numerical technique for one-dimensional thermal problems with phase-change. *International Journal of Heat and Mass Transfer*, 21(5), p.615.

Günther, E. et al., 2009. Enthalpy of Phase Change Materials as a Function of Temperature: Required Accuracy and Suitable Measurement Methods. *International Journal of Thermophysics*, 30(4), p.1257.

Hydro-Québec, 2006. *Réponses à la demande de renseignements no.2 de l'AQCIE/CIFQ*,

Ibánez, M. et al., 2005. An approach to the simulation of PCMs in building applications using TRNSYS. *Applied Thermal Engineering*, 25, pp.1796–1807.

Kuznik, F., Virgone, J. & Johannes, K., 2010. Development and validation of a new TRNSYS type for the simulation of external building walls containing PCM. *Energy and Buildings*, 42, pp.1004–1009.

Leduc, M.-A., Daoud, A. & Le Bel, C., 2011. Developing winter residential demand response strategies for electric space heating. In *12th Conference of International Building Performance Simulation Association (2011)*. Sydney, pp. 1111–1118.

Mehling, H. & Cabeza, L.F., 2008. *Heat and cold storage with PCM: An up to date introduction into basics and applications* D. Mewes & F. Mayinger, eds., Berlin: Springer.

Muruganantham, K., 2010. *Application of phase change material in buildings: field data vs. EnergyPlus simulation*. Arizona State University.

Pedersen, C.O., 2007. Advanced zone simulation in EnergyPlus: incorporation of variable properties and phase change material (PCM) capability. In *Building Simulation*. Beijing, pp. 1341–1345.

Sharma, A. et al., 2009. Review on thermal energy storage with phase change materials and applications. *Renewable and Sustainable Energy Reviews*, 13(2), pp.318–345. Available at: http://www.sciencedirect.com/science/article/pii/S1364032107001402.

Tabares-Velasco, P.C., Christensen, C. & Bianchi, M., 2012. Verification and validation of EnergyPlus phase change material model for opaque wall assemblies. *Building and Environment*, 54, pp.186–196.

Voller, V. & Cross, M., 1981. Accurate solutions of moving boundary problems using the enthalpy method. *International Journal of Heat and Mass Transfer*, 24(3), p.545.

Yao, M. & Chait, A., 1993. An alternative formulation of the apparent heat capacity method for phase change problems. *Numerical Heat Transfer, part B, Fundamentals*, 24(3), p.279.

Zalba, B. et al., 2003. Review on thermal energy storage with phase change: materials, heat transfer analysis and applications. *Applied Thermal Engineering*, 23(3), pp.251–283. Available at: http://www.sciencedirect.com/science/article/pii/S1359431102001928.